International Journal of Thermal Sciences 48 (2009) 2074–2079

Contents lists available at ScienceDirect

International Journal of Thermal Sciences

journal homepage: www.elsevier.com/locate/ijts

Two-phase flow patterns of nitrogen and nanofluids in a vertically capillary tube

Guo-Shan Wang*, Ran Bao

School of Mechanical Engineering, Shanghai Jiao Tong University, Shanghai 200240, PR China

ARTICLE INFO

Article history:
Received 2 July 2008
Received in revised form
3 March 2009
Accepted 26 March 2009
Available online 23 April 2009

Keywords:
Nanofluids
Two-phase flow
Flow pattern map
Capillary tube

ABSTRACT

Two-phase flow patterns of nitrogen gas and aqueous CuO nanofluids in a vertically capillary tube were investigated experimentally. The capillary tube had an inner diameter of 1.6 mm and a length of 500 mm. Water-based CuO nanofluid was a suspension consisted of water, CuO nanoparticles and sodium dodecyl benzol sulphate solution (SDBS). The mass concentration of CuO nanoparticles varied from 0.2 wt% to 2 wt%, while the volume concentration of SDBS varied from 0.5% to 2%. The gas superficial velocity varied from 0.1 m/s to 40 m/s, while the liquid superficial velocity varied from 0.04 m/s to 4 m/s. Experiments were carried out under atmospheric pressure and at a set temperature of 30 °C. Compared with conventional tubes, flow pattern transition lines occur at relatively lower water and gas flow velocities for gas–water flow in the capillary tube. While, flow pattern transition lines for gas–nanofluid flow occur at lower liquid and gas flow velocities than those for gas–water in the capillary tube. The effect of nanofluids on the two-phase flow patterns results mainly from the change of the gas–liquid surface tension. Concentrations of nanoparticles and SDBS have no effects on the flow patterns in the present concentration ranges.

1. Introduction

Nanotechnology has been widely used in traditional industries because materials with sizes of nanometers possess unique physical and chemical properties. Choi firstly utilized this technology in the heat transfer field and proposed the term of "nanofluids" [1]. A number of studies have been carried out to understand and describe different behaviors of nanofluids, such as their thermal conductivity [2,3], the convective heat transfer associated with the fluid flow and transfer phenomena [4,5] and pool boiling heat transfer [6,7]. Most researches have proved that the addition of nanoparticles can greatly increase the thermal conductivity. Therefore, these researches focused on the single-phase convective heat transfer of nanofluids in tubes to enhance the forced convective heat transfer by making use of the increased thermal conductivity.

For the heat transfer characteristics of the two-phase flow are related to the flow structure, research on flow pattern of nanofluids in micro/mini channels is necessary to understand such heat transfer process. Up to now, no investigation concerning the two-phase flow characteristics of nanofluids in vertical micro/mini channels have been reported. Since the change of the surface tension may be remarkable for nanofluids, it is anticipated that the two-phase flow characteristics of nanofluid–gas should differ from those of pure liquid–gas in micro/mini channels. Nanofluid two-phase flow is a new research frontier of nanotechnology. It has its challenge due to the very limited research in this area. A comprehensive review in this new research frontier was recently carried out by Cheng et al. [8] which specially deals with the current research status of nanofluid two-phase flows and the research needs in this important area.

Early detailed literature review of air–water flow regimes in small systems can be found in a report by Wilmarth and Ishii [9]. A literature review of two-phase flow patterns and boiling flow of mixtures in small channels was recently reported by Cheng and Mewes [10]. Even though considerable differences exist in defining two-phase flow patterns in vertical mini-scale channels, flow patterns generally consist of bubbly, slug, churn and annular flow in conventional channels. In recent decades, many works on two-phase flow pattern of air–water in vertically capillary channels have been reported. Galbiati and Andreini [11] experimentally investigated the two-phase flow pattern in capillary tubes having inner diameters of 0.5, 1.0 and 2.0 mm respectively. Mishima and Hibiki [12] studied the characteristics of air–water flow in small vertical tubes with inner diameters ranging from 1.05 to 4.08 mm. Flow regime, void fraction, rising velocity of slug bubbles and frictional pressure drops were measured. Ide et al. [13] reported the flow patterns and frictional pressure drops in air–water flow in a vertical capillary tube having an inner diameter of 0.9 mm. Zhao and Bi [14] studied the two-phase flow patterns of air–water in vertical

* Corresponding author. Tel./fax: +86 21 34206568.
E-mail address: gswang@sjtu.edu.cn (G.-S. Wang).

1290-0729/$ – see front matter © 2009 Elsevier Masson SAS. All rights reserved.
doi:10.1016/j.ijthermalsci.2009.03.016

Nomenclature

d	inner diameter of test tube, m
l_e	length of entrance, m
U_{GS}	gas superficial velocity, m s^{-1}
U_{LS}	liquid superficial velocity, m s^{-1}
V	volume rate, m^3/s
ρ	density, kg/m^3
υ	kinetic viscosity, m^2/s
η	viscosity, (kg/ms)
σ	surface tension (N/m)

Subscripts

G	vapor line
L	liquid line

capillary channels with triangular cross-section having hydraulic diameters ranging from 0.866 to 2.866 mm. Wongwises and Pipathattakul [15] carried out an experimental investigation on flow patterns, pressure drops and void fractions of gas–liquid two-phase flow in an inclined narrow annular channel. Although a number of studies on the flow patterns in mini channels were reported, the present understanding is still insufficient since these studies focused only on water and air. Up to now, the studies concerning the effects of nanofluids on the two-phase flow patterns in vertically capillary tube have never been carried out. Only a few researches investigated experimentally the effect of the surfactants in fluids on the two-phase flow characteristics in vertical tubes [16–18]. For capillary tubes, the effect of surface tension of liquid on the two-phase flow patterns is remarkable and cannot be ignored compared with those of gravity and inertia force, therefore, the flow patterns of nanofluids–gas two-phase flow in a capillary tube may be quite different from those of water–air two-phase flow in capillary tube. Therefore, flow patterns of nanofluids–gas in capillary tubes may be quite different from those of liquid–gas.

The present experiment focused on flow patterns of gas–nanofluid in a vertically capillary tube having an inner diameter of 1.6 mm and a length of 500 mm. The test gas was nitrogen. The test liquid is water-based nanoparticle suspension consisted of water, CuO nanoparticles and sodium dodecyl benzol sulphate solution (SDBS). Flow pattern maps of gas–water, gas–water/SDBS mixtures and gas–nanofluids were identified by visual observation and photographs of a high-speed camera, respectively. The effect of nanofluids on the two-phase flow patterns was illustrated and discussed.

2. Experimental apparatus and procedure

Fig. 1 shows the schematic of test apparatus. In the present study, nitrogen gas, instead of air, was used for preventing its pollution of the test tube. After the start up, high pressure nitrogen gas from a nitrogen gas supply passed through a regulating tank, an adjusting value, a pressure gauge, a mass flow meter and finally entered a gas–liquid mixing chamber. The mixing chamber was made of transparent Pyrex glass plates. By using an auxiliary heater in the regulating tank, the temperature of the nitrogen gas was increased to a predetermined value of 30 °C. The pressure in the liquid tank was kept at 800 kPa to provide a driving power. Liquid in the liquid tank passed through a mini mass flow controller, an adjusting valve, and finally entered the gas–liquid mixing chamber. Temperature of the liquid was also increased to the same 30 °C as the gas temperature by using an auxiliary heater in the water tank. In order to enhance the mixing of gas and liquid before entering the test tube, the mixing chamber was packed with fine plastic meshes.

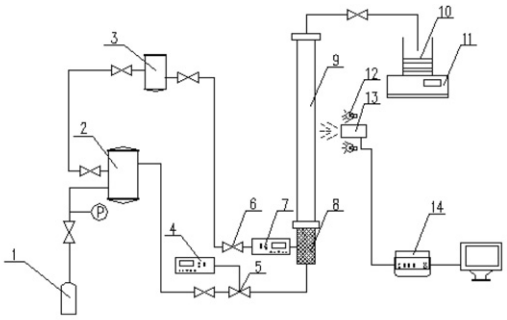

1. Gas cylinder 2. Gas tank 3. Liquid tank 4. Gas mass flow controller 5. Gas flow valve 6. Liquid flow valve 7. Liquid mass flow controller 8. Gas-Liquid mixing section 9. Test section 10. Liquid collection tank 11. Electronic balance 12. Lighting bulb 13. High-speed video camera 14. Data acquisition system

Fig. 1. Schematic diagram of experimental apparatus.

After that, the gas–liquid mixture flowed through the test tube and entered a collecting tank which was mounted on the outlet of the test tube. The gas was then separated and released into the atmosphere while the liquid drained into a glass cylinder.

Since the liquid mass rate was too low to measure directly with unerring precision, the liquid mass flow controller was only a monitor of the liquid mass rate. The collecting tank method was used for measuring the liquid mass rate. Liquid in the collecting tank finally flowed into a glass cylinder with the volume of 3 l which was placed on an electronic balance. The average liquid mass rate was indirectly obtained by measuring the weight increase of the cylinder in a time interval. Then, according to the mean inner diameter of test tube and the density of liquid, the liquid superficial velocity was determined indirectly. A volumetric flow meter was used for measuring the gas volume rate. The gas superficial velocity was calculated from the measured volume rate and the mean inner diameter of the test tube. A mean inner diameter was used while converting mass flow rate to the superficial velocity and the measured mean inner diameter was accurately 1.64 mm. Effect of densities of nanofluids with different concentrations has also been considered in calculation of the superficial velocity.

Fig. 2 shows the schematic of the test tube. The test tube was a Pyrex glass tube with an inner diameter of 1.6 mm and a length of

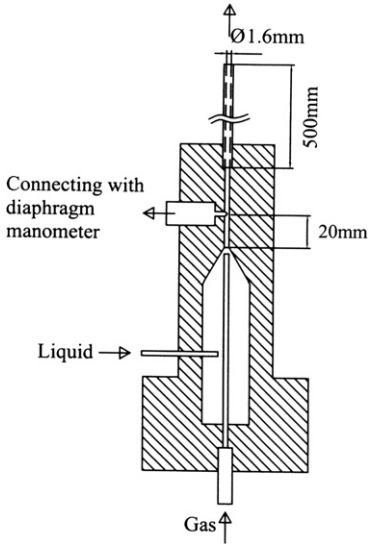

Fig. 2. Geometric diagram of the test section.

500 mm. At the inlet of the test tube, there was a transparent Pyrex rectification section with the same inner diameter as that of the test tube. A digital pressure transducer was mounted on it to measure pressure drops along the test tube and the pressure tap was located 50 mm away from the inlet of the test tube. The outlet of the test tube was connected to the collecting tank and opened in air.

Flow patterns were identified by visual observation and photographs of a high-speed camera. The observing point was in the center location of the test tube.

Fig. 3 shows a TEM morphology of the nanofluid with 1% CuO mass concentration. The nanofluid consisted of distilled water, surfactant of sodium dodecyl benzene sulphate (SDBS) and CuO nanoparticles. CuO nanoparticles were commercial products made by gas condensation and its average diameter was 50 nm. The mass concentration of CuO nanoparticles varied from 0.2 wt% to 2 wt% (333–3330 ppm), while the volume concentration of SDBS varied from 0.5% to 2% (5000–20 000 ppm). Before each test, the CuO nanoparticles, the surfactant and distilled water were put into and surged in an ultra-sonic water bath for about 12 h to get good suspension. The frequency is between 25 and 40 kHz. 12 h of oscillation is a conference time which can ensure fully dispersion. More time on oscillation had no effect on the nanofluid preparation and nanofluid properties. The physical properties of CuO nanofluids were directly measured in the present experiments. The surface tension was precisely measured using a direct optical measurement system based on the deferential capillary rise method [19].

Experimental conditions are given as follows: the inner diameter and the length of the test tube were 1.6 mm and 500 mm respectively. The gas superficial velocity varied from 0.1 m/s to 40 m/s, while the liquid superficial velocity varied from 0.04 m/s to 4 m/s. Experiments were carried out under atmospheric pressure and at a set temperature of 30 °C.

The gas superficial velocity and liquid superficial velocity are defined as below, respectively:

$$U_{GS} = V_G/(\pi d^2/4) \tag{1}$$

$$U_{LS} = V_L/(\pi d^2/4) \tag{2}$$

The absolute pressure was measured with an accuracy of 1%. The test tube mean diameter was measured by a liquid filling method and the accuracy was within 2.5%. The accuracies of gas superficial velocity and liquid superficial velocity were 3.5% and 6%, respectively.

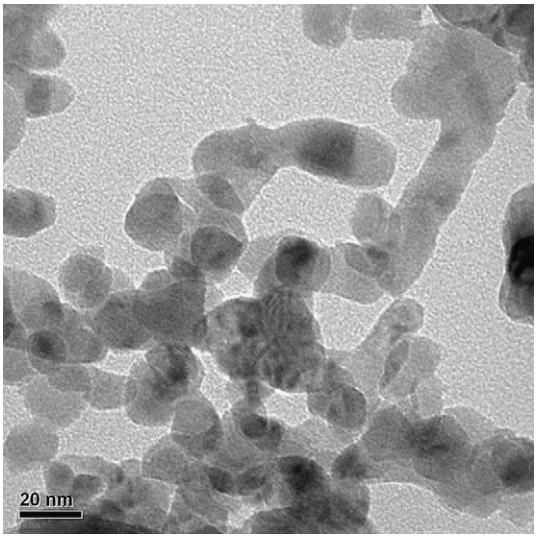

Fig. 3. TEM morphology of nanofluid with 1% CuO mass concentration.

3. Results and discussions

3.1. The flow patterns of gas–water two-phase flow

In this study, as two-phase flow of air–pure liquid in a vertical large-scale tube, four typical flow patterns including bubbly, slug, churn and annular flow could be identified when gas and nanofluids were used as working agents. Fig. 4 shows some typical flow regime photographs. Bubbly flow is usually characterized by the presence of distinct and discrete gas bubbles in the continuous liquid phase. Bubbles are usually sphere-like, generally smaller in diameter than the inner diameter of the test tube. Slug flow is characterized by elongated cylindrical bubbles. Gas slugs exist also in the continuous liquid phase, but gas slug has a semi-spherically shaped nose, a smooth body and a semi-spherically shaped nose tail. In churn flow, the continuous gas core occupies most of the tube cross-section, the liquid film forms at the sidewall. The gas phase and liquid phase has no distinct and smooth surface. The gas–liquid surface is rather irregular. Annular flow exists at high gas superficial velocities and the entire range of liquid superficial velocities. In annular flow, the continuous gas core occupies most of the tube cross-section and the liquid film forms at the sidewall. The most important criterion the difference of the froth flow and the annular flow is that the gas phase and liquid phase has distinct and smooth surface in the annular flow.

Fig. 5 shows the flow pattern map for upward flow of nitrogen–water in the vertical capillary tube. Abscissa and ordinate are the superficial velocities of gas and liquid, respectively. Various solid curves shown in Fig. 5 are the calculated flow pattern transition lines from the model by Taitel et al. [20] for predicating the conventionally large-scale vertical tubes.

The present experimental data are compared with those predicted by the model from Taitel et al. [20] in Fig. 5. Of course, it is impossible to get a complete agreement with the model used for conventional sizes. However, Fig. 5 can reveal clearly which flow regimes are significantly affected by the tube size.

The main transition criteria by Taitel model may be described as below [20]:

The bubble–slug transition line is;

$$U_{GS} + U_{LS} = 4.0\left[\frac{d^{0.429}(\sigma/\rho_L)^{0.089}}{\nu_L^{0.072}}\left(\frac{g(\rho_L-\rho_G)}{\rho_L}\right)\right] \tag{3}$$

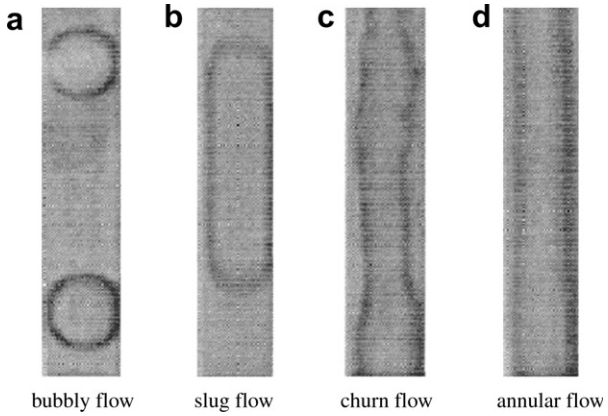

Fig. 4. Photographs of typical flow regime.

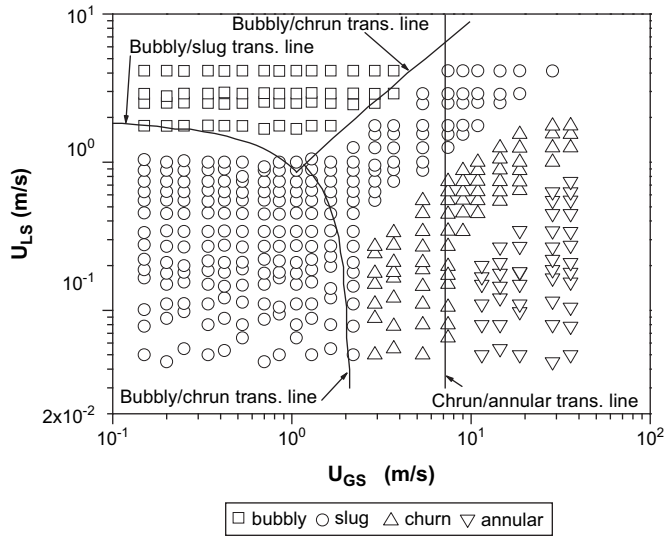

Fig. 5. Flow pattern map for gas–water upward flow compared with the model by Taitel.

$$\frac{U_{GS}}{U_{LS}+U_{GS}} > 0.52 \tag{4}$$

The slug–churn transition line is;

$$\frac{l_e}{d} = 40.6\left(\frac{U_{LS}+U_{GS}}{\sqrt{gd}} + 0.22\right) \tag{5}$$

The churn–annular transition line is;

$$\frac{U_{GS}\rho_G^{1/2}}{[\sigma g(\rho_L-\rho_G)]^{1/4}} = 3.1 \tag{6}$$

For the bubbly–slug transition lines, it is found that the experimental data of the bubbly flow regime are in reasonable agreement with the predicted results. But the gas velocities at bubbly–slug transition lines predicted by the model are higher than those of the experimental data.

For the slug–churn transition line, when the liquid superficial velocity is lower than 0.3 m/s, the experimental data of the slug–churn transition line agrees well with the predicted line. However, when it is higher than 0.3 m/s, the experimental results of the slug flow regime are reverse to the predicted line values.

For the churn–annular transition line, when the liquid superficial velocity is lower than 0.3 m/s, the experimental data of the churn–annular transition agree roughly with the predicted results. The churn–annular transition takes place at rather higher gas velocities than the predicted values. However, when the liquid superficial velocity is higher than 0.3 m/s, the experimental results drift off the predicted values.

The comparisons mentioned above show that the conventional size model can reasonably well predict the bubbly–slug flow transition. It can also roughly predict the slug–churn and churn–annular flow transitions when the liquid superficial velocity is lower than 0.3 m/s. However, it cannot be extended to predict slug–churn and churn–annular flow pattern transitions when the liquid superficial velocity is higher than 0.3 m/s. The reason should be that the effect of the surface tension on the flow patterns has not considered in the model, however, this effect cannot be neglected for capillary tube since the surface tension is of the same importability with gravity and inertia force.

3.2. The flow pattern map of gas–water/SDBS mixture flow

After adding SDBS and nanoparticles into distilled water, the main changes of physical properties of suspensions are the gas–liquid surface tension, viscosity and thermal conductivity. Thermal conductivity has no effect on the flow patterns according to the model by Taitel et al. [20]. According to the measured result in the present experiment, viscosity has only small change when distilled water is replaced by the mixtures (the change of viscosity is less than 5% for water/1% SDBS), therefore, the effect of viscosity is also small on various flow patterns. Therefore, the gas–liquid surface tension may be a governing parameter which causes the change of the flow patterns of nanofluids.

Fig. 6 shows the change of gas–liquid surface tension for both water/SDBS mixtures and nanofluids. The ordinate is ratio of the surface tension of nanofluids to that of water, and the abscissa is the mass concentration of nanofluids. Here, the measured surface tension of distilled water is 0.0712 N/m. It is found that the tensions of water/SDBS mixtures without nanoparticles decrease to about 75% of that of water and the volume concentration of SDBS has no effect on the surface tension in the present test range. Meanwhile, the surface tensions of nanofluids (mixtures of distilled water, surfactants and nanoparticles) are 63% of that of distilled water and the concentration of nanoparticles has no effect on the surface tension in the present test range. In addition, the surface tension of water/nanoparticles mixture without surfactant decreases gradually with increasing the nanoparticle mass concentration in the mass concentration range less than 1%. Then, it trends to a constant of 85% of that of water after the mass concentration exceeds 1%. It is clear that adding solely surfactant or adding solely nanoparticles into the base liquid will decrease the surface tension of the base fluid.

Cheng et al. [18] investigated the effect of the surfactant concentration on the surface tension of the working liquid. It is found that the surface tension decreases gradually with increasing the surfactant concentration in the very low volume concentration range, then, it trends a stable value when the volume concentration is over a critical value. This critical value varied in the range about from 100 ppm to 1000 ppm for different surfactants. Although different surfactants were used in their study, it seems that all surfactants possess such same characteristics. In the present work, the measured lowest volume concentration of the surfactant was 5000 ppm, therefore, the volume concentration of surfactant has no effect on the surface tension.

Fig. 7 shows the changes of the viscosities of nanofluids. The ordinate is the ratio of the viscosity of nanofluids to that of water,

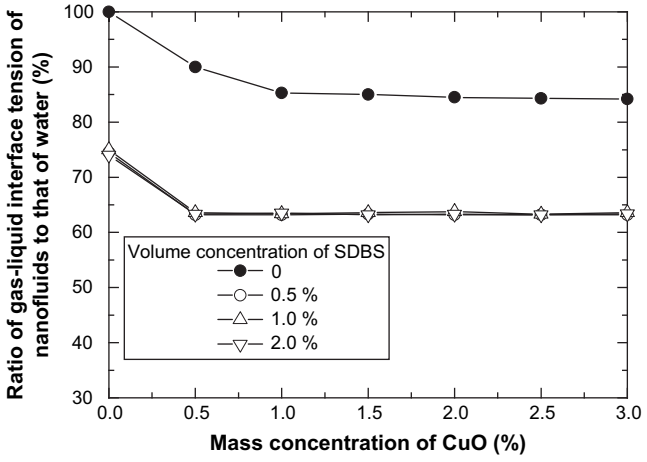

Fig. 6. Ratio of surface tensions of the nanofluids to distilled water.

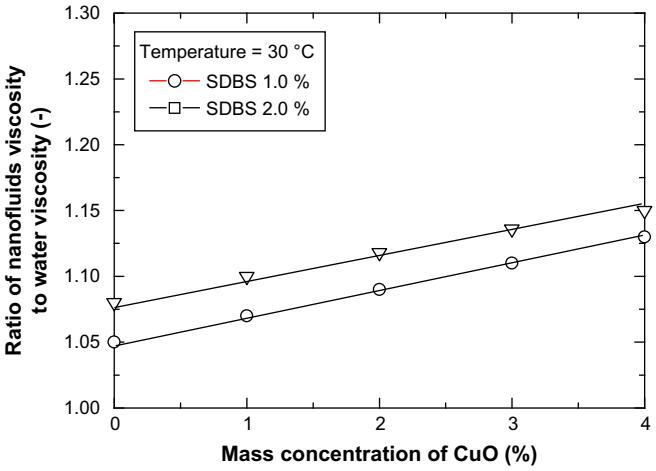

Fig. 7. Ratio of the viscosity of the nanofluids to distilled water.

and the abscissa is the mass concentration of nanofluids. It is found that the viscosity increases slowly with both increasing concentrations of SDBS and nanoparticles. Since the concentrations of nanoparticles and SDBS were small in the working liquids, the change of the viscosity was insignificant.

In order to investigate the influence of the surfactant or surface tension on flow patterns, Fig. 8 shows the plotted data of two-phase flow patterns for upward flow of nitrogen–water/1% SDBS mixture in the vertically capillary tube. The various solid curves shown in Fig. 8 are the calculated flow pattern transition lines from the model by Taitel et al. [20]. While, Fig. 9 illustrates the comparison of the flow pattern transitions lines of gas–water with those of gas–water/SDBS to understand more clearly the sole effect of the surface tension on the two-phase flow patterns.

For the bubbly–slug transition, since the surface tension of the water/SDBS mixture is lower than that of water, the transition lines of water/SDBS mixture significantly move further downward compared with that of water. The bubbly flow regime expends downward. For the slug–churn flow transition, the transition line of water/SDBS mixture moves further leftward significantly compared with that of water when the liquid superficial velocity is lower than 0.3 m/s. Therefore, the slug flow regime becomes narrower than

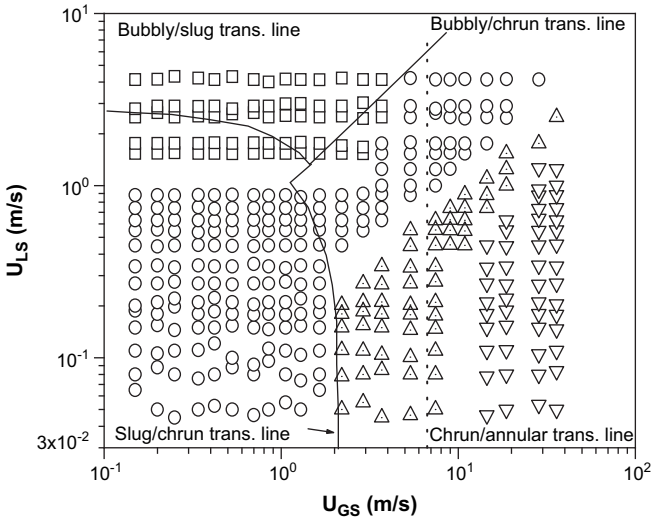

Fig. 8. Flow pattern map for nitrogen–water SDBS mixture compared with the model by Taitel.

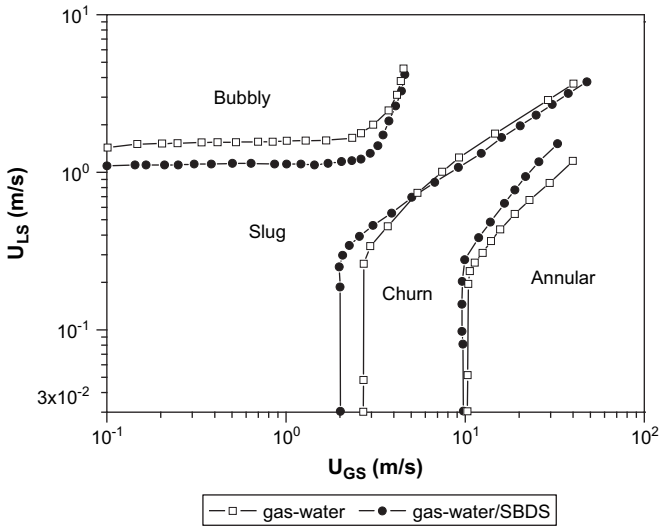

Fig. 9. Comparisons of flow pattern transitions between gas–water and gas–water/SDBS.

those of the gas–water due to the decease of the surface tension. For the churn–annular transition, the transition line of water/SDBS mixture is almost the same as that of water when the liquid superficial velocity is lower than 0.3 m/s. Therefore, the effect of the gas–liquid surface tension on the two-phase flow patterns has great relation with the liquid superficial velocity.

The reason why the surface tension affects the slug–churn transition can be explained as follows: the surface tension causes the system to minimize its interfacial area, which helps to maintain spherical shapes of bubbles. This can keep the fluids together in the tube thus retarding the transition from slug to annular flow.

3.3. The flow patterns of gas–nanofluids two-phase flow

Fig. 10 shows the plotted data of flow patterns for upward flow of nitrogen–nanofluids with 1 wt% CuO particles in the vertical capillary tube. The various solid curves shown in Fig. 10 are the calculated flow pattern transition lines from the model by Taitel, Bornea and Dukler [20]. Additional, Fig. 11 illustrates the comparison among the flow pattern transition lines of gas–water, gas–

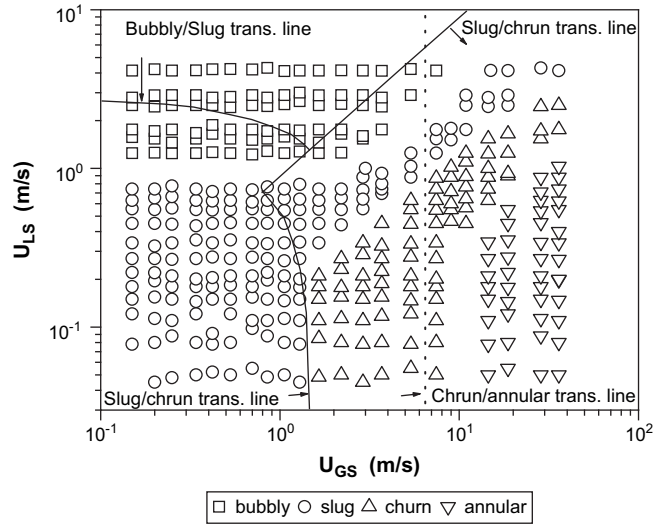

Fig. 10. Flow pattern map for nitrogen–nanofluid compared with the model by Taitel.

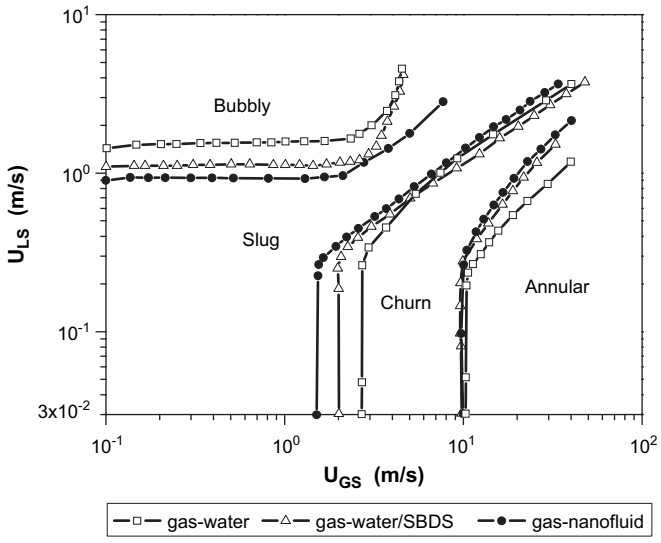

Fig. 11. Comparisons of the flow pattern transitions among nitrogen–nanofluid, nitrogen–water/SDBS mixture and nitrogen–water.

water/SDBS and gas–nanofluid to understand more clearly the differences of the flow pattern transition lines for the three liquids. It should be noted that the nanoparticle concentration has almost no effect on the flow patterns of nanofluids since the surface tensions of nanofluids have no almost relations with the particle concentration in the present concentration range as shown in Fig. 6. Therefore, only the flow pattern map of the nanofluid with the mass concentration of 1 wt% is illustrated.

For the bubbly–slug transition, since the surface tension of the nanofluid is lower than that of the water/SDBS mixture, the transition lines of gas–nanofluid significantly move further downward and rightward compared with that of gas–water/SDBS mixture. The bubbly flow regime expends downward and rightward. For the slug–churn flow transition, the transition line moves further leftward significantly compared with that of the gas–water/SDBS mixture when the liquid superficial velocity is lower than 0.3 m/s. Therefore, the slug flow regime becomes narrower than those of the gas–water and the gas–water/SDBS mixture due to the decrease of the surface tension. For the churn–annular transition, the transition line is almost the same as that of the gas–water/SDBS mixture when the liquid superficial velocity is lower than 0.3 m/s.

The present study is only a start stage for the nanofluid two-phase flow. For further study, the effects of the size, kind and concentration of nanoparticles on the surface tension and the flow patterns should be systemically investigated. Meantime, the theoretical model should also be developed to describe the two-phase flow characteristics when the surface tension is an important factor.

4. Conclusions

An experimental investigation was carried out to investigate the two-phase flow patterns of nitrogen–water, nitrogen–water/SDBS mixture and nitrogen–aqueous nanofluids in a vertical capillary tube with an inner diameter of 1.60 mm and a length of 500 mm. The mass concentration of CuO nanoparticles varied from 0.2 wt% to 2 wt%, while the volume concentration of SDBS varied from 0.5 % to 2%. The gas superficial velocity varied from 0.1 m/s to 40 m/s, while the liquid superficial velocity varied from 0.04 m/s to 4 m/s. Experiments were carried out under atmospheric pressure and at a set temperature of 30 °C.

There are relatively slight differences between the flow pattern maps of gas–nanofluids and gas–water. These differences may result from the change of surface tension, while these differences have no relation with both of the nanoparticles concentrations and SDBS concentrations in the base liquid.

The bubbly–slug transition of the nitrogen–nanofluid moves further downward and rightward compared with that of nitrogen–water. For nitrogen–nanofluid flow, when the liquid superficial velocity is lower than 0.3 m/s, the slug–churn transition moves significantly leftward compared with that of nitrogen–water and the churn–annular transition is basically same with that of nitrogen–water. When the liquid superficial velocity is higher than 0.3 m/s, the slug–churn transition is basically same with that of nitrogen–water and the churn–annular transition moves significantly leftward compared with that of nitrogen–water.

References

[1] S.U.S. Choi, Enhancing thermal conductivity of fluids with nanoparticles, in: Proceedings of the 1995 ASME Int. Mechanical Engineering Congress and Exhibition, San Francisco, CA, USA, 1995.
[2] S. Lee, S.U.S. Choi, S. Li, J.A. Eastman, Measuring thermal conductivity of fluids containing oxide nanoparticles, Journal of Heat Transfer, Transaction ASME 121 (1999) 280–289.
[3] B.X. Wang, L.P. Zhou, X.P. Peng, A fractal model for predicting the effective thermal conductivity of liquid with suspension of nanoparticles, International Journal of Heat and Mass Transfer 46 (2003) 2665–2672.
[4] Y.M. Xuan, Q. Li, Heat transfer enhancement of nanofluids, International Journal of Heat and Fluid Flow 2 (2001) 58–64.
[5] Y.M. Xuan, Q. Li, Investigation on convective heat transfer and flow features of nanofluids, Journal of Heat Transfer, Transaction ASME 125 (2003) 151–155.
[6] S.K. Das, N. Putra, W. Roetzel, Pool boiling characteristics of nanofluids, International Journal of Heat and Mass Transfer 46 (2003) 851–862.
[7] Z.H. Liu, J.G. Xiong, R. Bao, Boiling heat transfer characteristics of nanofluids in a flat heat pipe evaporator with micro-grooved heating surface, International Journal of Multiphase Flow 33 (2007) 1284–1295.
[8] L. Cheng, P. Bandarra Filho Enio, R. Thome John, Nanofluid two-phase flow and thermal physics: a new research frontier of nanotechnology and its challenges, International Journal of Nanoscience and Nanotechnology 8 (2008) 3315–3332.
[9] T. Wilmarth, M. Ishii, Two-phase flow patterns in narrow rectangular vertical and horizontal channels, International Journal of Heat and Mass Transfer 37 (1994) 1749–1758.
[10] L. Cheng, D. Mewes, Review of two-phase flow and flow boiling of mixtures in small and mini channels, International Journal of Multiphase Flow 32 (2006) 183–207.
[11] L. Galbiati, P. Andreini, Flow pattern transition for vertical downward two-phase flow in capillary tubes, International Journal of Heat and Mass Transfer 19 (1992) 791–799.
[12] K. Mishima, T. Hibiki, Some characteristics of air–water two-phase flow in small diameter vertical tubes, International Journal of Multiphase Flow 22 (1996) 703–712.
[13] H. Ide, H. Matsumura, Y. Tanaka, Y. Fukano, Flow patterns and frictional pressure drop in gas–liquid two-phase flow in vertical capillary channels with rectangular cross-section, Transaction JSME 63 (1997) 452–460.
[14] T.S. Zhao, Q. Bi, Co-current air–water two-phase flow patterns in vertical triangular microchannels, International Journal of Multiphase Flow 27 (2001) 765–782.
[15] S. Wongwises, K. Pipathattakul, Flow patterns, pressure drops and void fraction of two-phase gas–liquid in an inclined narrow annular channel, Experimental Thermal and Fluid Science 30 (2006) pp. 345–354.
[16] Rozenblit, et al., Flow patterns and heat transfer in vertical air–water flow with surfactant, International Journal of Multiphase Flow 32 (2006) 889–901.
[17] Z.H. Liu, Y.P. Gao, Effect of surfactant on two-phase flow patterns of water-gas in capillary tubes, Journal of Hydrodynamics Series B 19 (2007) 630–634.
[18] L. Cheng, D. Mewes, A. Luke, Boiling phenomena with surfactants and polymeric additives: a state-of-the-art review, International Journal of Heat and Mass Transfer 50 (2007) 2744–2771.
[19] J.T. Wu, Z.G. Liu, F.K. Wang, C. Ren, Surface tension of dimethyl: from 213 to 368 K, Journal of Chemical and Engineering Data 48 (2003) 1571–1573.
[20] Y. Taitel, D. Bornea, A.E. Dukler, Modeling flow pattern transitions for steady upward gas–liquid flow in vertical tubes, AIChE Journal 26 (1980) 345–354.